

Boost-DiLeu: Enhanced Isobaric N,N-Dimethyl Leucine Tagging Strategy for Comprehensive Quantitative Glycoproteomic Analysis

Danqing Wang,^{1,#} Min Ma,^{2,#} Junfeng Huang,² Ting-Jia Gu,² Yusi Cui,¹ Miyang Li,¹ Zicong Wang,² Henrik Zetterberg,^{3,4,5,6,7} Lingjun Li^{1,2*}

¹Department of Chemistry, University of Wisconsin-Madison, Madison, WI 53706, USA.

²School of Pharmacy, University of Wisconsin-Madison, Madison, WI 53705, USA.

³Institute of Neuroscience and Physiology, Sahlgrenska Academy, University of Gothenburg, Gothenburg, S-431 80, Gothenburg, Sweden.

⁴Clinical Neurochemistry Laboratory, Sahlgrenska University Hospital, S-431 80, Mölndal, Sweden.

⁵Department of Molecular Neuroscience, UCL Institute of Neurology, Queen Square, London, WC1N 3BG, UK.

⁶UK Dementia Research Institute at UCL, London, WC1N 3BG, UK.

⁷Hong Kong Center for Neurodegenerative Diseases, Hong Kong, China.

[#]These authors contributed equally.

*To whom correspondence should be addressed.

E-mail: lingjun.li@wisc.edu. Phone: (608)-265- 8491, Fax: (608)-262-5345. Mailing Address: 5125 Rennebohm Hall, 777 Highland Avenue, Madison, WI 53705

Abstract

Intact glycopeptide analysis has been of great interest because it can elucidate glycosylation site information and glycan structural composition at the same time. However, mass spectrometry (MS)-based glycoproteomic analysis is hindered by the low stoichiometry of glycosylation and poor ionization efficiency of glycopeptides. Due to the relatively large amounts of starting materials needed for enrichment, identification and quantification of intact glycopeptides in some size-limited biological systems are especially challenging. To overcome these limitations, here we developed an improved boosting strategy to enhance N,N-dimethyl leucine tagging-based quantitative glycoproteomic analysis, termed as Boost-DiLeu. With integration of one-tube sample processing workflow and high pH fractionation, 3514 quantifiable N-glycopeptides were identified from 30 μ g HeLa cell tryptic digests with reliable quantification performance. Furthermore, this strategy was applied to human cerebrospinal fluid (CSF) samples to differentiate N-glycosylation profiles between Alzheimer's disease (AD) patients and non-AD donors. The results revealed processes and pathways affected by dysregulated N-glycosylation in AD, including platelet degranulation, cell adhesion, and extracellular matrix, which highlighted the involvement of N-glycosylation aberrations in AD pathogenesis. Moreover, co-expression network analysis (WGCNA) showed 3 modules of glycoproteins, one of which are associated with AD phenotype. Our results demonstrated the feasibility of using this strategy for comprehensive glycoproteomic analysis of size-limited clinical samples. Taken together, we developed and optimized a strategy for enhanced comprehensive quantitative intact glycopeptide analysis with DiLeu labeling, which is especially promising for identifying novel therapeutic targets or biomarkers in sample size limited models or systems.

Introduction

Glycosylation is one of the most common post-translational modifications (PTMs), which is involved in many physiological processes including cell signaling, host-pathogen interaction, and immune response.¹ Studies have shown aberrant glycosylation plays a key role in the pathological processes during disease progression, such as neurodegenerative diseases, diabetes, and cancers.²⁻⁵ Intact glycopeptide analysis has been of great interest recently because it retains information of glycosylation sites while elucidating peptide sequences and glycan structures, which enables the investigation of functional effects of heterogeneity across glycoproteome.⁶ However, akin to many other PTMs, mass-spectrometry (MS)-based glycoproteomic analysis has been hindered by the low abundance of glycosylation in biological samples and poor ionization efficiency of glycopeptides.^{7,8}

To overcome these limitations, various enrichment strategies have been developed to separate glycopeptides from other non-glycosylated peptides in biological samples before MS analysis.² For example, hydrophilic interaction liquid chromatography (HILIC) has been extensively used to enrich glycopeptides based on their increased hydrophilicity introduced by glycan moieties.⁹⁻¹¹ However, even utilizing these highly efficient enrichment methods, comprehensive glycoproteomic analysis still requires a relatively large amount of starting sample. This drawback particularly limits glycoproteomic analysis of precious clinical samples such as pathological tissues and cerebrospinal fluid (CSF), which cannot be expanded in vitro and are often limited in quantities for research.¹²

On the other hand, insufficient MS signal intensity from low abundance peptides usually leads to low proteome coverage in LC-MS/MS analysis, because the poor-quality MS/MS spectra can hardly generate confident peptide identifications. Isobaric labeling can be used to enhance MS detection sensitivity in data-dependent acquisition (DDA) mode analysis, since the signal intensities of precursor ions in the full scan are combined from all labeling channels of the same species¹³ Abundant peptide backbone fragments and enhanced signal intensities in MS/MS facilitate identification while achieving multiplex quantification at the same time. Recent studies have taken advantage of isobaric labeling and introduced the concept of “boosting” (or “carrier”) channel, in which a large amount of content-relevant sample is labeled by one channel of the isobaric tags and combined with those size-limited samples labeled by the rest channels. The combined signal intensity of a given peptide can be greatly amplified and thus enhancing the detection of low-abundance peptide, as well as mitigating sample loss of the samples labeled with much less amount during sample preparation.^{13,14} Such strategy has been applied to single-cell proteomics,^{15,16} quantification of phosphopeptides,¹³ phosphotyrosine-containing peptides,¹⁶ deglycosylated peptides of secreted glycoproteins,¹⁷ stable isotope labeling using amino acids in cell culture (SILAC)-labeled peptides,¹⁸ and low-abundant proteins in thermal proteome profiling (TPP).¹⁹ These studies showed promising features of boosting approach to increase the proteome coverage and enable quantification of low-abundant proteins/peptides at the same time, which would be especially useful for PTM analysis of size-limited samples. Nonetheless, such strategy has not been applied to intact glycopeptide analysis yet.

Our group previously developed N,N-Dimethyl Leucine (DiLeu) isobaric tags for quantitative proteomics analysis, where the amine-reactive group selectively reacted with N-termini and lysine residues of peptides similar to TMT²⁰ and isobaric tags for relative and absolute quantification (iTRAQ)²¹. Compared to these commercially available tags, DiLeu is much more cost-effective, which can be synthesized in-house readily at high yield.²² It was first designed as a 4-plex set²³ and then expanded to 8-plex.²⁴ Incorporating neutron encoding (NeuCode) strategy, 12-plex set²² and 21-plex set²⁵ were achieved lately.²⁵ In 12-plex DiLeu setting, reporter ions are grouped into four regions ranging from 115 *m/z* to 118 *m/z*, and the mass difference of adjacent channel is as small as 6 mDa within each region.²² DiLeu tag¹³ is well-suited for developing a boosting strategy for intact glycopeptides, since it has been successfully applied to intact glycoproteomic quantification on cell line and tissue samples in our previous studies.^{9,26} More importantly, it possesses higher multiplex capacity and is less likely to be affected by the isotopic impurity “leakage” problem reported for 10-plex tandem mass tags (TMT).^{1323242225229,26}

In this study, we developed 12-plex DiLeu tag based boosting strategy (Boost-DiLeu) to perform comprehensive quantitative N-glycoproteomic analysis on size-limited samples (Figure 1). To further recover glycopeptides from small-sized samples, we adapted a one-tube processing strategy¹² for DiLeu labeling, leveraging the benefits of an acid-cleavable detergent, RapiGest SF Surfactant (Waters Corporation) to circumvent the necessities of sample desalting. The strategy was well established by carefully optimizing sample handling process, boosting-to-study channel (B/S) ratios, and instrumental parameters for data acquisition including automatic gain control (AGC) and ion injection time (IT). Coupling with HILIC enrichment and high-pH (HpH) reversed-phase liquid chromatography (RPLC) fractionation, large-scale global mapping of N-glycoproteome were achieved from a small amount of HeLa cell digests. To further demonstrate the feasibility of strategy for size-limited clinical sample analysis, we applied Boost-DiLeu to profile the N-glycoproteomic changes in cerebrospinal fluid (CSF) between Alzheimer’s disease (AD) patients and healthy donors. Taken together, the Boost-DiLeu strategy not only increased the glycoproteome coverage, but also succeed in accurate and robust quantification, which shed light on future applications to site-specific quantitative glycoproteomic studies involving size-limited samples.

Experimental Section

Chemicals. Dithiothreitol (DTT), sequencing grade trypsin were from Promega (Madison, WI). Optimal LC/MS grade solvents, Tris base, urea, and sodium chloride were from Fisher Scientific (Pittsburgh, PA). Trifluoroacetic acid (TFA), iodoacetamide (IAA), triethylammonium bicarbonate (TEAB), sodium dodecyl sulfate (SDS), N,N-dimethylformamide (DMF), 4-(4,6-dimethoxy-1,3,5-triazin-2-yl)-4-methylmorpholinium tetrafluoroborate (DMTMM), and dimethyl sulfoxide (DMSO) were purchased from Sigma-Aldrich (St Louis, MO). N-methylmorpholine (NMM) was purchased from TCI America (Tokyo, Japan). Oasis HLB 1 cc (10 mg) extraction cartridges and RapiGest SF (RapiGest) were purchased from Waters Corporation (Milford, MA). Hydroxylamine solution was purchased from Alfa Aesar (Ward Hill, MA). Strong anion exchange (SAX) bulk material PolySAX LP (12 μ m, 300 \AA) and strong cation exchange (SCX) spin tips were obtained

from PolyLC (Columbia, MD). Empty TopTips were from Glygen Corp (Columbia, MD). Protease inhibitor cocktail tablets and phosphatase inhibitor cocktail tablets were from Roche (Mannheim, Germany).

HeLa Cell Sample Preparation. Details of cell culture and sample preparation with conventional method are provided in Supporting Information. In one-tube sample processing workflow, HeLa cell pellets were solubilized in 0.1% (w/v) RapiGest prepared in 100 mM TEAB with 1% (v/v) protease inhibitor and phosphatase inhibitor. The mixture was then heated at 60 °C for 30 min and sonicated at 4 °C for 1 min. Lysates were centrifuged at 21000 g at 4 °C for 5 min and the supernatant was collected. Protein BCA assay, reduction, alkylation, and trypsin digestion were performed in the same way as mentioned in the conventional method. After digestion, peptides were dried down *in vacuo* without acidification and desalting.

CSF Sample Preparation. CSF samples were collected by lumbar puncture from five male AD patients and five male non-AD patients. The samples were from patients who sought medical advice because of cognitive impairment. Patients were designated as AD and non-AD according to CSF biomarker levels using cutoffs that are >90% specific for AD (PMID: 16488378): total-tau (T-tau) >350 pg/mL, phospho-tau 181 (P-tau181) >60 pg/mL and Aβ42 <530 pg/mL (2 out 3 positive). None of the biochemically normal subjects fulfilled these criteria. Detailed subjects' information is provided in Supplemental Table S1. The study was approved by the regional ethics committee at the University of Gothenburg. Protein concentration was determined by BCA protein assay. 30 µg proteins were aliquoted for each study channels. 900 µg proteins pooled from both AD patients and healthy donors CSF samples were used as boosting channel. The aliquots were dried down *in vacuo* and treated with the one-tube sample preparation approach as described above.

DiLeu Labeling. DiLeu tags synthesis and labeling were performed as previously reported.^{22,26} Briefly, DiLeu tags were activated in anhydrous DMF with DMTMM and NMM at 0.6x molar ratios to tags. The mixture was vortexed at room temperature for 1h and the supernatant was then added to each sample for labeling. After vortexing at room temperature for 2 h, the reaction was quenched by adding 5% NH₂OH to a final concentration of 0.25%. Each batch of labeled peptides were pooled together and dried down *in vacuo*.

SAX-HILIC Enrichment. Enrichment of DiLeu-labeled glycopeptides was performed with in-house packed SAX-HILIC SPE tips following previous publications with minor modification.^{26,27} Briefly, 3 mg of cotton wool was plugged into a 200 µL empty TopTip, which was placed on a 2 mL microcentrifuge tube with the help of an adapter unit. SAX bulk material was activated in 1% TFA and vortexed for 15 min. The SAX slurry was transferred into the cotton-packed TopTip at a beads-to-peptide ratio of 30:1. Solvent was removed at 200 g for 2 min. The stationary phase was conditioned with 200 µL 1% TFA and 300 µL loading buffer (80% ACN/1% TFA) for three times. The DiLeu-labeled sample was dissolved in 300 µL loading buffer and loaded onto the SAX-cotton tip. The tip was centrifuged at 200 g for 2 min and flow-through of was reloaded to the SAX-cotton for four more times to ensure complete retention. The SAX-cotton tip was washed with 300 µL loading buffer for six times, and then eluted with 150µL 0.1% FA solution for three times. Samples

were dried down *in vacuo* before direct MS analysis or HpH fractionation.

Off-Line HpH Fractionation. HpH fractionation was performed on a Waters Alliance e2695 HPLC using a 150 mm x 2.1 mm, 5mm, 100 Å, C18 column (Phenomenex) operating at 0.2 mL/min. Mobile phase A was 10 mM ammonium formate in water (pH 10) and mobile phase B was 10 mM ammonium formate in 90% acetonitrile (ACN) (pH 10). Separation was performed with the following gradient: 1% B (0–5 min), 1–40% B (5–50 min), 40–60% B (50–54 min), 60–70% B (54–58 min), and 70–100% B (58–59 min). Fractions were collected every 4 minutes and 14 fractions were collected in total. Nonadjacent fractions were concatenated into 4 tubes for MS analysis.

LC-MS/MS Analysis. Lyophilized samples reconstituted in 0.1% FA were loaded onto a 15 cm length, 75 µm i.d. in-house packed Bridged Ethylene Hybrid C18 (1.7 µm, 130 Å, Waters) column, and analyzed on an Orbitrap Fusion Lumos Tribrid mass spectrometer (Thermo Fisher Scientific, San Jose, CA) interfaced with a Dionex UltiMate 3000 UPLC system (Thermo Fisher Scientific, San Jose, CA). Two technical replicates were run for each fraction. For intact N-glycopeptides analysis, the LC gradient was from 0 to 30% ACN (0.1% FA) for 80 min. Survey scans of peptide precursors from m/z 400 to 2000 were performed at resolving power of 120 K and AGC target of 4E5 with a maximum IT of 100 ms. For MS2 scan, a duty cycle of 3s was set in top speed mode. Only spectra with a charge state among 2-7 were selected for fragmentation by higher-energy collision dissociation (HCD) with normalized collision energy (NCE) of 30 and \pm 3% stepped HCD. The MS2 spectra were acquired with a resolution of 60 K, lower mass limit of 110 m/z, and dynamic exclusion of 12 s with 10 ppm mass tolerance. Different AGC settings and maximum ITs were tested for method optimization. AGC 3E4 and a maximum IT 200 ms were used for final analysis. For global proteomic analysis, details are provided in Supporting Information.

Data Analysis. Raw files were searched against UniProt Homo sapiens reviewed database (August 2020, 20311 sequences) using Byonic search engine (version 2.9.38, Protein Metrics Inc) embedded within Proteome Discoverer 2.1 (PD 2.1) (Thermo Fisher Scientific). Trypsin was selected as the enzyme and two maximum missed cleavages were allowed. Searches were performed with a precursor mass tolerance of 15 ppm and a fragment mass tolerance of 0.03 Da. Static modifications were specified as carbamidomethylation (+57.02146 Da) on cysteine residues and 12-plex DiLeu (+145.12801 Da) on peptide N-terminus and lysine residues. Dynamic modifications consisted of oxidation of methionine residues (+15.99492 Da), deamidation (+0.984016 Da) of asparagine and glutamine residues, and N-glycosylation. Oxidation and deamidation were set as “rare” modification, and N-glycosylation was set as “common” modification. Glycan modifications were searched against a glycan database expanded from the Byonic embedded human N-glycan database (182 entries) to include mannose-6-phosphate (M6P) glycans consisting of HexNAc (2-4) Hex (3-9) Phospho (1-2) modification. N-glycopeptides were filtered at a 1% peptide FDR, Byonic score >150 and $\log|\text{Prob}| > 1$. Proteins were filtered at a 1% protein FDR for global proteomic analysis. Glycopeptides were exclusively categorized into six glycosylation type categories based on the glycan composition identified: (1) M6P (containing M6P glycan); (2) sialylated (containing sialic acid); (3) fucosylated (containing fucose); (4)

complex/hybrid (> 2 HexNAc); (5) high mannose (2 HexNAc and > 5 Hex), and (5) paucimannose (2 HexNAc and < 5 Hex). Quantification of protein and N-glycopeptides was performed in PD 2.1 with a reporter ion integration tolerance of 10 ppm for the most confident centroid. Reporter ion intensities were exported, and isotopic interference correction was performed in a Python script according to the previously described equations.²² Reporter ion intensity of each channel was normalized by median to correct systematic biases of 12 -plex DiLeu tags via Perseus.²⁸ Student's t-test was performed, where significant change was defined by a p-value less than 0.05 and fold-change over 1.5 .²⁸ Gene ontology analysis was conducted using Database for Annotation, Visualization and Integrated Discovery (DAVID) version 6.8 .²⁹ Protein-protein interaction network was generated by Metascape and Cytoscape.^{30,31} WGCNA algorithm was used for network analysis and details are provided in Supporting Information.³²

Results and Discussion

One-tube Sample Processing Workflow for DiLeu Labeled Glycoproteomics. In conventional isobaric labeling sample preparation workflow, 4% SDS lysis buffer and urea solution are commonly used. Since SDS is detrimental for MS and urea can interfere with DiLeu labeling, extensive steps are required to remove them. This is usually tedious and time-consuming, which impedes experimental efficiency and reproducibility. Moreover, they can introduce decent amount of sample loss.³⁰ Such issue becomes more severe when a study aims to analyze low-abundance PTMs. Recently, Wu et al introduced a strategy termed as Nanogram TMT Processing in One Tube (NanoTPOT) to achieve desalt-free isobaric labeling using TMT tag in a single tube.¹² An acid-cleavable detergent, RapiGest SF Surfactant, was utilized to alleviate the need for desalting. Here we adapted and optimized this strategy to conduct desalting-free DiLeu labeling. To assess the performance of this optimized one-tube DiLeu labeling sample processing, same amount of HeLa cell pellet was processed both in conventional method and this method. In conventional sample preparation workflow, cells were lysed in lysis buffer containing 4% SDS and proteins were extracted through organic solvent precipitation. The protein precipitate was then redissolved in 8M urea solution to perform reduction, alkylation, and trypsin digestion, and afterwards the peptides were desalted before DiLeu tag labeling. In the optimized one-tube sample preparation workflow, cells were lysed in lysis buffer containing 0.1% RapiGest and the supernatant was collected to perform reduction, alkylation, and trypsin digestion directly without extra steps of precipitation and urea buffer resuspension. After digestion, the sample was dried down and labeled with DiLeu tags without desalting. SDS-PAGE result suggested that the trypsin digestion was complete in both methods (Figure S1). In terms of proteome coverage, both workflows identified comparable number of labeled peptides in global proteome analysis (Figure S2A) and there was an overlap of 66% identified proteins between these two methods (Figure S2B). For DiLeu labeled glycoproteomics, the one-tube sample processing method outperformed the conventional one in all aspects, including identification of glycopeptide-spectrum matches (GPSMs), unique glycopeptides and corresponding glycoproteins (Figure 2A). Among all identified glycoproteins, 57.1% were found in both methods, while 13.8% more unique glycoproteins were identified in one-tube sample processing method (Figure 2B). The outstanding performance of the one-tube

sample processing method may attribute to two reasons: (1) RapiGest was a preferred reagent for handling membrane proteins and the protein precipitation step was skipped since there is no need to remove RapiGest after extraction.³³ (2) Avoid desalting before labeling effectively reduced sample loss, especially for hydrophilic glycopeptides. Taken together, the one-tube sample processing strategy is suitable for DiLeu labeled glycoproteomic analysis.

Evaluation of Boost-DiLeu strategy. In the Boost-DiLeu strategy, the analysis of small-sized samples labeled with study channels was enhanced by utilizing a boosting channel that contains a much larger number of labeled glycopeptides from analogous biological samples. After pooled together, isobaric labeled glycopeptides from each channel appeared as a single precursor ion at MS1 level, and the existence of boosting channel greatly increased the intensity of the precursor ion and helped to trigger MS2 fragmentation. To validate the design of the Boost-DiLeu strategy and evaluate the effects of different boosting-to-study channel (B/S) ratios on glycoproteomic coverage and quantification, a series of comparison was performed using HeLa cell tryptic digests prepared with one-tube sample processing workflow. The first three channels (115a, 115b, and 116a) in 12-plex DiLeu were set as study channels and loaded with 10 µg tryptic peptides respectively. The last channel, DiLeu 118d, was selected as the boosting channel to generate different B/S ratios at 30x, 50x, and 100x (Figure 3A). A control group was prepared at the same time that only consisted of the first three study channels. Each group of samples was pooled together after labeling and enriched through HILIC before LC-MS/MS analysis.

DiLeu 118d was selected as the boosting channel because the reporter ion in this channel had no interference with other channels. Its -1 isotopic peak (²H to ¹H) caused by isotopic impurity was at m/z 117.14656, which was 3mDa away from the DiLeu 12-plex 117c reporter ion at m/z 117.14363. Such mass difference can be resolved using high-resolution power during LC/MS-MS analysis. Figure 3B displayed the reporter ion signal intensity distribution at a 30x B/S ratio. Similar reporter ion intensity distribution in study channels were observed and none of the empty channels had unusually high reporter ion signal, indicating that 118d channel successfully served as a boosting channel and avoided the isotopic interference problem reported in 10-plex TMT tags,¹³ which ensured high quantification accuracy and maximum multiplex capacity of DiLeu tags.

Figure 3C demonstrated the effectiveness of adding a boosting channel, as the quantifiable glycopeptides in study channels, which stand for glycopeptides without missing reporter ion intensities, increased three times at B/S 30x compared to the control group. As expected, the identified number of GPSMs went up from 2132 to 2370 as the B/S ratios increased. However, the unique glycopeptide number and the quantifiable glycopeptides dropped as the B/S ratios increased. Simultaneously, an increased median coefficient of variations (CVs) from 13.41% to 28.19% (Figure 3D) was observed, which show a similar trend reported in other studies.^{13,16} Since total number of ions entering the Orbitrap was controlled in each scan, ions from boosting channel were likely to occupy more space than ions in study channels. At a higher B/S ratio, the signal intensity of reporter ions from study channels was suppressed (Figure S3). Lower reporter ion signal intensity negatively affected the quantification performance, including more missing values found in 50x and 100x groups and increased median coefficient of variations (CVs) from 13.41%

to 28.19% (Figure 3D). The same comparison was also made at three different B/S ratios using samples prepared with conventional method (Figure S4). Despite of the lower identification number, a similar trend of fewer quantifiable glycopeptides and higher median of CVs was observed with the increase of B/S ratios, suggesting that 30x boosting ratio was optimal in aspect of identification and quantification accuracy.

Optimization of Instrument Parameters. When performing MS/MS analysis, the number of precursor ions reaching to orbitrap analyzer is controlled by AGC setting and maximum IT. These parameters are essential to balance the detection sensitivity and MS2 scan rate. For global proteomic analysis, AGC is usually set in the range of 5E4 to 1E5 to improve the overall coverage.¹⁶ However, such setting may not be well-suited for PTM analysis due to its low stoichiometry, especially in the case where a large portion of boosting samples are mixed with study samples. Ions from boosting sample can fill in the analyzer quickly, thus impairing the detection of signals from study channels. To understand the influence of AGC settings on glycoproteome coverage and quantification quality, and find out an optimal value, four different AGC settings including 5E3, 3E4, 5E4 and 5E5 were compared with DiLeu-labeled HeLa cell tryptic digests with a 30x boosting channel added as described in previous section. The maximum IT was fixed at 200 ms. In general, a higher AGC setting allows more ions to accumulate for MS/MS analysis at expense of MS2 scan rate and longer duty cycle time, thus affecting proteome coverage.^{16,34} Such trend was observed in Figure 4A, where AGC 3E4 achieved the highest identification numbers of GPSMs, glycopeptides, and quantifiable glycopeptides while higher AGC values led to decreasing identification numbers. As reflected in Figure 4B, the median of IT increased from 18 ms to 200 ms when increasing AGC values. The lowest AGC setting 5E3 got significantly poorer glycoproteome coverage, indicating the necessity of allowing enough ions to enter the orbitrap for high-quality MS/MS analysis. On the other hand, accumulating more ions improves quantification quality since more ions from study channels are allowed to enter the mass analyzer.^{16,35} Though the reporter ion intensity decreased slightly at higher AGC settings due to potential space charge effects³⁶ or preference of fragmentation on glycosidic bonds (Figure 4C), the median of CV distribution decreased from 23.63% to 12.97% (Figure 4D).

Along with the AGC settings, maximum IT is another important parameter to control the number of ions for MS2 analysis. To find out an optimal setting, two different maximum IT at 200 ms and 300 ms were evaluated with the same B/S ratio of 30x and AGC setting of 5E4. As shown in Figure S5A, increased IT elongated duty cycle time, thus resulting in lower identification numbers. In terms of quantification performance, the distribution of reporter ion signal intensity (Figure S5B) and CVs (Figure S5C) were almost similar in both cases, despite that 200 ms IT had a slightly lower median of CV of 16.61% than 17.71% of 300 ms IT setting.

These results clearly demonstrated a trade-off between glycoproteome coverage and quantification performance at different AGC settings. Higher AGC improved quantification quality at expense of number of identified glycopeptides. Maximum IT also had great impact on glycoproteome coverage, while the influence on quantification performance was not as significant as AGC settings. To achieve a balance between glycoproteome coverage and quantification quality,

AGC 3E4 and maximum IT 200 ms were implemented in Boost-DiLeu strategy for glycoproteomics analysis.

Global Glycoproteome Mapping in HeLa Cell Line. HpH fractionation has been widely applied in proteomic analysis to provide an additional dimension of separation with conventional low-pH RPLC due to its high orthogonality and compatibility with direct MS analysis.³⁷ Recently, several studies reported that integrating HpH fractionation into PTM sample preparation workflow after enrichment largely bolstered the proteome coverage of those low-abundance samples.^{13,38-40} However, additional separation requires a sufficient amount of sample to compensate for potential sample loss during the process, and this is usually unsuitable for small-sized samples. With the Boost-DiLeu strategy, a larger amount of boosting sample can serve as a “carrier” sample that mitigate the impact of sample loss.⁴¹ Therefore, HpH fractionation was implemented in the Boost-DiLeu strategy to further boost the glycoproteome coverage. Similar to previous evaluation experiment, 30 µg HeLa tryptic digest peptides were labeled in the first three study channels and a boosting channel at B/S ratio of 30x was added. The samples went through HpH fractionation after HILIC enrichment. In total, 4119 glycopeptides from 277 proteins were identified within the four fractions, among which 3514 were quantifiable (Figure 5A, Table S2). Glycoproteome coverage was expanded at approximately 2.5-fold compared to samples analyzed without additional HpH fractionation. Figure 5B displayed the overlap of glycopeptides identified in four fractions, and 29.62%, 15.36%, 17.56% and 23.64% of glycopeptides were unique in each fraction, indicating the complementary orthogonality provided by HpH fractionation. In conventional HILIC enrichment, fractionation is usually performed based on the decreasing ACN content.^{9,26} Though glycopeptides eluted successively based on their hydrophilicity, it was found that most of the glycopeptides came out at the first two fractions with only a small portion of glycopeptides eluting in the latter two fractions.⁴² In contrast, utilization of HpH fractionation greatly improved the efficiency of separation. Such comprehensive intact glycoproteome coverage also enabled global profiling site-specific micro-heterogeneity of HeLa cell glycosylation, as visualized by a glycoprotein-glycan network diagram (Figure 5C). The outer nodes displayed all identified glycans, while the inner bar represented corresponding glycoproteins with different number of glycosylation sites. Of note, more than half of the glycoproteins had only one glycosylation site, but 79.1% of glycosites have more than one glycan. In addition, several glycosylation patterns were observed, such as prevalence of high mannose glycosylation (44.11% of glycopeptides). Complex/hybrid and fucosylated glycans were more likely to occur on protein with multiple glycosites. Interestingly, 34 glycans were found to be M6P glycans out of total 151 glycan compositions. Due to the negatively charged phosphate group and extremely hydrophilic property, detection of M6P glycopeptides usually suffers interference from other N-glycopeptides.⁴³ With HpH fractionation, M6P glycopeptides were better separated from other glycopeptides so the detection sensitivity was enhanced. Along with improved glycoproteome coverage, the Boost-DiLeu strategy also presented good quantification quality after HpH fractionation. Figure 5D showed the median intensities of study channels were close to 1:1:1 without any isotopic interference from the DiLeu 118d channel. CV median of 16.75% (Figure 5E) and average Pearson correlation over 0.97 (Figure 5F) among three biological replicates evidenced the robustness and

accuracy of quantification in this strategy.

Applying Boost-DiLeu strategy to CSF samples. CSF plays an essential role in brain development, neural functioning, and regulating brain interstitial fluid homeostasis.³⁸ Since it is the only body fluid that directly interchanges with the extracellular fluid of central nervous system (CNS), it can directly reflect pathological changes in the CNS.⁴⁴⁻⁴⁶ However, the analysis of CSF samples is challenging due to the limited amount of sample collected from each donor and the relatively low total protein concentration (0.2 - 0.8 mg/mL).⁴⁷ The intrinsic low amount of glycosylation in biological samples makes the analysis even harder, as glycopeptides only take up a small portion of total peptide mixtures (2% to 5%).³⁸ As designed to address such challenges, Boost-DiLeu strategy was adopted to profile glycoproteomic changes in CSF between AD patients and healthy donors. 30 µg of tryptic peptides from CSF samples obtained from five AD patients and five healthy donors were labeled with DiLeu tag in each study channel. The boosting channel of 30x B/S ratio was pooled from CSF samples of AD patients and healthy donors at a ratio of 3:5 due to the limited size of AD CSF samples. Besides glycoproteomic analysis, conventional proteomics analysis was performed using an aliquot of labeled samples to ensure that the observed change in glycopeptide level was not resulted from protein-level regulation. In total, 1321 intact N-glycopeptides were identified, and 1172 of them were quantifiable, mapping to 164 glycoproteins and 158 different glycans (Figure S6A, Table S3). Figure S6B shows the glycoprotein-glycan network of all quantifiable glycopeptides. Nearly 62% of the glycoproteins were observed with only one glycosite, yet 47% of the glycosites were modified with more than one glycan. In the meantime, 5% of glycoproteins were found to have more than 4 glycosylation sites. This result suggested the high degree of glycoproteome heterogeneity in CSF samples and the necessity of intact glycoproteomic analysis. Among all quantifiable glycopeptides, 49% and 22% of them were sialylated and fucosylated, and the prevalence of these two glycosylation types was also in line with previously reported label-free study of N-glycopeptides in CSF samples.³⁸

Compared to healthy controls, 22 glycopeptides were found significantly changed, with 9 up-regulated and 9 down-regulated with a fold-change over 1.5 (Figure 6A, Figure S7A). The corresponding 14 glycoproteins were not observed to dysregulate in the parallel proteomics analysis, suggesting that the dysregulation of glycopeptides came exclusively from PTM level (Figure S7B). Notably, 72% of these glycopeptides were sialylated and 38% were fucosylated, which further emphasized the significance of the two types of glycosylation on the pathogenesis of AD.^{3,48} GO analysis showed that these dysregulated glycoproteins were significantly enriched in platelet degranulation, reverse cholesterol transport, cell adhesion and complement activation, which have been reported to be associated with neuronal degeneration in AD (Figure S7D).⁴⁹⁻⁵² Majority of dysregulated glycoproteins in AD were localized at extracellular region, in accordance with the fact that CSF is in direct contact with the extracellular space of the brain and many N-glycoproteins are secreted proteins (Figure S7E).^{53,54} Protein-protein interaction network indicated that these proteins were mainly related to platelet degranulation and response to elevated platelet cytosolic Ca²⁺ (Figure S7C). Platelet degranulation was reported to play a pivotal role in platelet-mediated amyloid-β (Aβ) oligomerization in AD, which is believed to be greatly relevant to disease

progression.^{55,56} Alterations in calcium homeostasis is found to be critically implicated in brain aging and the neuropathology of AD, and the involvement of glycoproteins with response to elevated platelet cytosolic Ca^{2+} may provide deeper insight into the role of cytosolic calcium level during the progression of AD.^{57,58} Among these glycoproteins, four up-regulated sialyl glycopeptides were observed at two sites of prostaglandin-H2 D-isomerase (PTHDS, Uniprot accession: P41222), a protein that involves in multiple CNS functions and acts as a chaperone for preventing the formation of neurotoxic agents such as $\text{A}\beta$ fibrils.⁵⁹ This suggests that aberrant sialylation on this protein might play a specific role in AD progression through accelerated $\text{A}\beta$ aggregation.⁶⁰

To further study individual N-glycoproteome organization in CSF and its alternations in AD, WGCNA analysis was applied to construct an N-glycoproteomic network. Three modules (ME) with similar expression patterns were identified via average linkage hierarchical clustering and one module (M1) showed significant negative correlation with AD (Figure 6B). The corresponding clinical traits of individuals showed significant positive correlation with AD at Tau and Ptau level, while opposite correlation was found at abeta level (Figure S8A). Subsequently, we performed network analysis based on the continuous measure of membership and connectivity to determine the top 30 hub glycoproteins in M1 (Figure S8B). GO enrichment uncovered that M1 was closely associated with the biological process of extracellular matrix organization, axon guidance, and was mainly involved in extracellular related cellular functions (Figure 6C, Table S4).

Conclusions

Here we successfully set up a robust and highly sensitive strategy, Boost-DiLeu for enhanced isobaric labeled quantitative intact glycoproteomic analysis. Utilizing one-tube sample processing workflow, several sample preparation steps were eliminated, and all sample handling processes were completed in a single tube. This sample preparation method not only simplified experimental steps, but also greatly reduced sample loss and increased proteome coverage of DiLeu labeled samples. During labeling, we utilized a boosting channel consisting of relatively large amounts of biological samples analogous to samples of interest in study channels to further increase glycoproteome coverage and enhance quantification performance. B/S ratio of 30x was found to be optimal in both aspect of identification and quantification accuracy. MS2 parameters including AGC settings and maximum IT were optimized, and a trade-off between glycoproteome coverage and quantification accuracy was observed. As a compromise, 3E4 AGC and 200 ms IT were suggested as a starting point. Additional HpH fractionation after conventional HILIC enrichment provided complementary orthogonality in separation, which further boosted glycoproteome coverage. As a proof-of-principle experiment, the Boost-DiLeu strategy was applied to the site-specific N-glycoproteome analysis of human CSF samples from AD patients and healthy donors. Overall, 1172 quantifiable intact glycopeptides were identified from 164 glycoproteins, and 18 glycopeptides were found to be dysregulated. WGCNA analysis revealed one module of proteins significantly negatively correlated with AD. These results demonstrated the feasibility of using this strategy for glycoproteomic analysis on size-limited clinical samples., which would be essential for future biomarker discovery and development of personalized

medicine. Notably, while we developed the Boost-DiLeu strategy with the 12-plex DiLeu tag set in this study, similar strategy may also be adapted to the 21-plex DiLeu tag for higher multiplex capacity without apparent isotopic interference from boosting channel.²⁵ Future implementation of this strategy could also expand to other DiLeu labeled PTM analyses on small-sized biological samples, such as phosphorylation and citrullination.

Supporting Information

The Supporting Information is available free of charge on the ACS Publications website:

Data availability; figure of SDS-PAGE; figures of proteomic-level comparison of two sample preparation method; figure of distribution of reporter ion intensities at different B/S ratios; figures of comparison of different B/S ratios; figures of different maximum IT setting comparison; figures of site-specific quantitative glycoproteomic analysis of human CSF samples. Table of CSF subject information; table of quantifiable glycopeptides in HeLa cell; table of quantifiable glycopeptides in CSF; table of GO analysis result of M1 proteins.

Author Information

Corresponding author. Email: lingjun.li@wisc.edu

Notes

H.Z. has served at scientific advisory boards and/or as a consultant for Abbvie, Alector, Annexon, AZTherapies, CogRx, Denali, Eisai, Nervgen, Pinteon Therapeutics, Red Abbey Labs, Passage Bio, Roche, Samumed, Siemens Healthineers, Triplet Therapeutics, and Wave, has given lectures in symposia sponsored by Cellecrticon, Fujirebio, Alzecure and Biogen, and is a co-founder of Brain Biomarker Solutions in Gothenburg AB (BBS), which is a part of the GU Ventures Incubator Program (outside submitted work). The other authors declare no conflict of interest.

Acknowledgements

This work was supported, in part, by the National Institutes of Health Grants U01CA231081, RF1AG052324, and R01 DK071801 (to L.L.). The Orbitrap instruments were purchased through the support of an NIH Shared Instrument Grant (NIH-NCRR S10RR029531 to L.L.) and the University of Wisconsin-Madison, Office of the Vice Chancellor for Research and Graduate Education with funding from the Wisconsin Alumni Research Foundation. L.L. acknowledges a Vilas Distinguished Achievement Professorship and Charles Melbourne Johnson Distinguished Chair Professorship with funding provided by the Wisconsin Alumni Research Foundation and University of Wisconsin-Madison School of Pharmacy. H.Z. is a Wallenberg Scholar supported by grants from the Swedish Research Council (#2018-02532), the European Research Council (#681712), Swedish State Support for Clinical Research (#ALFGBG-720931), the Alzheimer Drug Discovery Foundation (ADDF), USA (#201809-2016862), the AD Strategic Fund and the Alzheimer's Association (#ADSF-21-831376-C, #ADSF-21-831381-C and #ADSF-21-831377-C), the Olav Thon Foundation, the Erling-Persson Family Foundation, Stiftelsen för Gamla Tjänarinnor, Hjärnfonden, Sweden (#FO2019-0228), the European Union's Horizon 2020

research and innovation programme under the Marie Skłodowska-Curie grant agreement No 860197 (MIRIADE), and the UK Dementia Research Institute at UCL.

Reference

- (1) Delafield, D. G.; Li, L. Recent Advances in Analytical Approaches for Glycan and Glycopeptide Quantitation. *Mol. Cell Proteomics* **2021**, *20*, 100054.
- (2) Chen, Z.; Huang, J.; Li, L. Recent Advances in Mass Spectrometry (MS)-Based Glycoproteomics in Complex Biological Samples. *Trends Analyt Chem.* **2018**, *118* (Cell 126 2006), 880–892.
- (3) Fang, P.; Xie, J.; Sang, S.; Zhang, L.; Liu, M.; Yang, L.; Xu, Y.; Yan, G.; Yao, J.; Gao, X.; Qian, W.; Wang, Z.; Zhang, Y.; Yang, P.; Shen, H. Multilayered N-Glycoproteome Profiling Reveals Highly Heterogeneous and Dysregulated Protein N-Glycosylation Related to Alzheimer’s Disease. *Anal. Chem.* **2019**, *92* (1), 867–874.
- (4) Hu, Y.; Pan, J.; Shah, P.; Ao, M.; Thomas, S. N.; Liu, Y.; Chen, L.; Schnaubelt, M.; Clark, D. J.; Rodriguez, H.; Boja, E. S.; Hiltke, T.; Kinsinger, C. R.; Rodland, K. D.; Li, Q. K.; Qian, J.; Zhang, Z.; Chan, D. W.; Zhang, H.; Consortium, C. P. T. A.; Pandey, A.; Paulovich, A.; Hoofnagle, A.; Zhang, B.; Mani, D. R.; Liebler, D. C.; Ransohoff, D. F.; Fenyo, D.; Tabb, D. L.; Levine, D. A.; Kuhn, E.; Whiteley, F. M.; Whiteley, G. A.; Zhu, H.; Shih, I.-M.; Bavarva, J.; McDermott, J. E.; Whiteaker, J.; Ketchum, K. A.; Clauser, K. R.; Ruggles, K.; Elburn, K.; Ding, L.; Hannick, L.; Zimmerman, L. J.; Watson, M.; Thiagarajan, M.; Ellis, M. J. C.; Oberti, M.; Mesri, M.; Sanders, M. E.; Borucki, M.; Gillette, M. A.; Snyder, M.; Edwards, N. J.; Vatanian, N.; Rudnick, P. A.; McGarvey, P. B.; Mertins, P.; Townsend, R. R.; Thangudu, R. R.; Smith, R. D.; Rivers, R. C.; Slebos, R. J. C.; Payne, S. H.; Davies, S. R.; Cai, S.; Stein, S. E.; Carr, S. A.; Skates, S. J.; Madhavan, S.; Liu, T.; Chen, X.; Zhao, Y.; Wang, Y.; Shi, Z. Integrated Proteomic and Glycoproteomic Characterization of Human High-Grade Serous Ovarian Carcinoma. *Cell Rep.* **2020**, *33* (3), 108276.
- (5) Tang, L.; Chen, X.; Zhang, X.; Guo, Y.; Su, J.; Zhang, J.; Peng, C.; Chen, X. N-Glycosylation in Progression of Skin Cancer. *Med. Oncol.* **2019**, *36* (6), 50.
- (6) Riley, N. M.; Hebert, A. S.; Westphall, M. S.; Coon, J. J. Capturing Site-Specific Heterogeneity with Large-Scale N-Glycoproteome Analysis. *Nat. Commun.* **2019**, *10* (1), 1–13.
- (7) Nwosu, C. C.; Strum, J. S.; An, H. J.; Lebrilla, C. B. Enhanced Detection and Identification of Glycopeptides in Negative Ion Mode Mass Spectrometry. *Anal. Chem.* **2010**, *82* (23), 9654–9662.

(8) Hart-Smith, G.; Raftery, M. J. Detection and Characterization of Low Abundance Glycopeptides Via Higher-Energy C-Trap Dissociation and Orbitrap Mass Analysis. *J. Am. Soc. Mass Spectrom.* **2012**, *23* (1), 124–140.

(9) Chen, Z.; Yu, Q.; Hao, L.; Liu, F.; Johnson, J.; Tian, Z.; Kao, W. J.; Xu, W.; Li, L. Site-Specific Characterization and Quantitation of N-Glycopeptides in PKM2 Knockout Breast Cancer Cells Using DiLeu Isobaric Tags Enabled by Electron-Transfer/Higher-Energy Collision Dissociation (EThcD). *Analyst* **2018**, *143* (11), 2508–2519.

(10) Mysling, S.; Palmisano, G.; Højrup, P.; Thaysen-Andersen, M. Utilizing Ion-Pairing Hydrophilic Interaction Chromatography Solid Phase Extraction for Efficient Glycopeptide Enrichment in Glycoproteomics. *Anal. Chem.* **2010**, *82* (13), 5598–5609.

(11) Qing, G.; Yan, J.; He, X.; Li, X.; Liang, X. Recent Advances in Hydrophilic Interaction Liquid Interaction Chromatography Materials for Glycopeptide Enrichment and Glycan Separation. *Trends Anal. Chem.* **2020**, *124*, 115570.

(12) Wu, R.; Pai, A.; Liu, L.; Xing, S.; Lu, Y. NanoTPOT: Enhanced Sample Preparation for Quantitative Nanoproteomic Analysis. *Anal. Chem.* **2020**, *92* (9), 6235–6240.

(13) Yi, L.; Tsai, C.-F.; Dirice, E.; Swensen, A. C.; Chen, J.; Shi, T.; Gritsenko, M. A.; Chu, R. K.; Piehowski, P. D.; Smith, R. D.; Rodland, K. D.; Atkinson, M. A.; Mathews, C. E.; Kulkarni, R. N.; Liu, T.; Qian, W.-J. Boosting to Amplify Signal with Isobaric Labeling (BASIL) Strategy for Comprehensive Quantitative Phosphoproteomic Characterization of Small Populations of Cells. *Anal. Chem.* **2019**, *91* (9), 5794–5801.

(14) Slavov, N. Single-Cell Protein Analysis by Mass Spectrometry. *Curr. Opin. Chem. Biol.* **2021**, *60*, 1–9.

(15) Budnik, B.; Levy, E.; Harmange, G.; Slavov, N. SCoPE-MS: Mass Spectrometry of Single Mammalian Cells Quantifies Proteome Heterogeneity during Cell Differentiation. *Genome Biol.* **2018**, *19* (1), 161.

(16) Tsai, C.-F.; Zhao, R.; Williams, S. M.; Moore, R. J.; Schultz, K.; Chrisler, W. B.; Pasatolic, L.; Rodland, K. D.; Smith, R. D.; Shi, T.; Zhu, Y.; Liu, T. An Improved Boosting to Amplify Signal with Isobaric Labeling (IBASIL) Strategy for Precise Quantitative Single-Cell Proteomics. *Mol. Cell Proteomics* **2020**, *19* (5), 828–838.

(17) Suttipitugsakul, S.; Tong, M.; Sun, F.; Wu, R. Enhancing Comprehensive Analysis of Secreted Glycoproteins from Cultured Cells without Serum Starvation. *Anal. Chem.* **2021**.

(18) Klann, K.; Tascher, G.; Münch, C. Functional Translatome Proteomics Reveal Converging and Dose-Dependent Regulation by MTORC1 and EIF2 α . *Mol. Cell* **2020**, *77* (4), 913–925.e4.

(19) Justice, S. A. P.; McCracken, N. A.; Victorino, J. F.; Qi, G. D.; Wijeratne, A. B.; Mosley, A. L. Boosting Detection of Low-Abundance Proteins in Thermal Proteome Profiling Experiments by Addition of an Isobaric Trigger Channel to TMT Multiplexes. *Anal. Chem.* **2021**, *93* (18), 7000–7010.

(20) Thompson, A.; Schäfer, J.; Kuhn, K.; Kienle, S.; Schwarz, J.; Schmidt, G.; Neumann, T.; Mohammed, A.; Hamon, C. Tandem Mass Tags: A Novel Quantification Strategy for Comparative Analysis of Complex Protein Mixtures by MS/MS. *Anal. Chem.* **2003**, *75* (8), 1895–1904.

(21) Ross, P.; Huang, Y.; Marchese, J.; Williamson, B.; Parker, K.; Hattan, S.; Khainovski, N.; Pillai, S.; Dey, S.; Daniels, S.; Purkayastha, S.; Juhasz, P.; Martin, S.; Bartlet-Jones, M.; He, F.; Jacobson, A.; Pappin, D. Multiplexed Protein Quantitation in *Saccharomyces Cerevisiae* Using Amine-Reactive Isobaric Tagging Reagents. *Mol. Cell. Proteomics* **2004**, *3* (12), 1154–1169.

(22) Frost, D. C.; Greer, T.; Li, L. High-Resolution Enabled 12-Plex DiLeu Isobaric Tags for Quantitative Proteomics. *Anal. Chem.* **2015**, *87* (3), 1646–1654.

(23) Xiang, F.; Ye, H.; Chen, R.; Fu, Q.; Li, L. N,N-Dimethyl Leucines as Novel Isobaric Tandem Mass Tags for Quantitative Proteomics and Peptidomics. *Anal. Chem.* **2010**, *82* (7), 2817–2825.

(24) Frost, D. C.; Greer, T.; Xiang, F.; Liang, Z.; Li, L. Development and Characterization of Novel 8-plex DiLeu Isobaric Labels for Quantitative Proteomics and Peptidomics. *Rapid Commun. Mass Spectrom.* **2015**, *29* (12), 1115–1124.

(25) Frost, D. C.; Feng, Y.; Li, L. 21-Plex DiLeu Isobaric Tags for High-Throughput Quantitative Proteomics. *Anal. Chem.* **2020**, *92* (12), 8228–8234.

(26) Dieterich, I. A.; Cui, Y.; Braun, M. M.; Lawton, A. J.; Robinson, N. H.; Peotter, J. L.; Yu, Q.; Casler, J. C.; Glick, B. S.; Audhya, A.; Denu, J. M.; Li, L.; Puglielli, L. Acetyl-CoA Flux from the Cytosol to the ER Regulates Engagement and Quality of the Secretory Pathway. *Sci. Rep.* **2021**, *11* (1), 2013.

(27) Cui, Y.; Yang, K.; Tabang, D. N.; Huang, J.; Tang, W.; Li, L. Finding the Sweet Spot in ERLIC Mobile Phase for Simultaneous Enrichment of N-Glyco and Phosphopeptides. *J. Am. Soc. Mass Spectrom.* **2019**, 1–11.

(28) Tyanova, S.; Temu, T.; Sinitcyn, P.; Carlson, A.; Hein, M. Y.; Geiger, T.; Mann, M.; Cox, J. The Perseus Computational Platform for Comprehensive Analysis of (Proteo)Omics Data. *Nat. Methods* **2016**, *13* (9), 731–740.

(29) Huang, D. W.; Sherman, B. T.; Lempicki, R. A. Systematic and Integrative Analysis of Large Gene Lists Using DAVID Bioinformatics Resources. *Nat. Protoc.* **2009**, *4* (1), 44–57.

(30) Zhou, Y.; Zhou, B.; Pache, L.; Chang, M.; Khodabakhshi, A. H.; Tanaseichuk, O.; Benner, C.; Chanda, S. K. Metascape Provides a Biologist-Oriented Resource for the Analysis of Systems-Level Datasets. *Nat. Commun.* **2019**, *10* (1), 1523.

(31) Shannon, P.; Markiel, A.; Ozier, O.; Baliga, N. S.; Wang, J. T.; Ramage, D.; Amin, N.; Schwikowski, B.; Ideker, T. Cytoscape: A Software Environment for Integrated Models of Biomolecular Interaction Networks. *Genome Res.* **2003**, *13* (11), 2498–2504.

(32) McKenzie, A. T.; Moyon, S.; Wang, M.; Katsyv, I.; Song, W.-M.; Zhou, X.; Dammer, E. B.; Duong, D. M.; Aaker, J.; Zhao, Y.; Beckmann, N.; Wang, P.; Zhu, J.; Lah, J. J.; Seyfried, N. T.; Levey, A. I.; Katsel, P.; Haroutunian, V.; Schadt, E. E.; Popko, B.; Casaccia, P.; Zhang, B. Multiscale Network Modeling of Oligodendrocytes Reveals Molecular Components of Myelin Dysregulation in Alzheimer’s Disease. *Mol. Neurodegener.* **2017**, *12* (1), 82.

(33) Wu, F.; Sun, D.; Wang, N.; Gong, Y.; Li, L. Comparison of Surfactant-Assisted Shotgun Methods Using Acid-Labile Surfactants and Sodium Dodecyl Sulfate for Membrane Proteome Analysis. *Anal. Chim. Acta* **2011**, *698* (1–2), 36–43.

(34) Randall, S. M.; Cardasis, H. L.; Muddiman, D. C. Factorial Experimental Designs Elucidate Significant Variables Affecting Data Acquisition on a Quadrupole Orbitrap Mass Spectrometer. *J. Am. Soc. Mass Spectrom.* **2013**, *24* (10), 1501–1512.

(35) Specht, H.; Slavov, N. Optimizing Accuracy and Depth of Protein Quantification in Experiments Using Isobaric Carriers. *J. Proteome Res.* **2020**, *20* (1), 880–887.

(36) Dabrowski, R.; Ripa, R.; Latza, C.; Annibal, A.; Antebi, A. Optimization of Mass Spectrometry Settings for Steroidomic Analysis in Young and Old Killifish. *Anal. Bioanal. Chem.* **2020**, *412* (17), 4089–4099.

(37) Yang, F.; Shen, Y.; Camp, D. G.; Smith, R. D. High-PH Reversed-Phase Chromatography with Fraction Concatenation for 2D Proteomic Analysis. *Expert Rev. Proteom* **2014**, *9* (2), 129–134.

(38) Chen, Z.; Yu, Q.; Yu, Q.; Johnson, J.; Shipman, R.; Zhong, X.; Huang, J.; Asthana, S.; Carlsson, C.; Okonkwo, O.; Li, L. In-Depth Site-Specific Analysis of N-Glycoproteome in

Human Cerebrospinal Fluid and Glycosylation Landscape Changes in Alzheimer's Disease. *Mol. Cell Proteomics* **2021**, *20*, 100081.

(39) Fang, P.; Ji, Y.; Silbern, I.; Doebele, C.; Ninov, M.; Lenz, C.; Oellerich, T.; Pan, K.-T.; Urlaub, H. A Streamlined Pipeline for Multiplexed Quantitative Site-Specific N-Glycoproteomics. *Nat. Commun.* **2020**, *11* (1), 5268.

(40) Song, C.; Ye, M.; Han, G.; Jiang, X.; Wang, F.; Yu, Z.; Chen, R.; Zou, H. Reversed-Phase-Reversed-Phase Liquid Chromatography Approach with High Orthogonality for Multidimensional Separation of Phosphopeptides. *Anal. Chem.* **2010**, *82* (1), 53–56.

(41) Cheung, T. K.; Lee, C.-Y.; Bayer, F. P.; McCoy, A.; Kuster, B.; Rose, C. M. Defining the Carrier Proteome Limit for Single-Cell Proteomics. *Nat. Methods* **2020**, 1–8.

(42) Huang, J.; Liu, X.; Wang, D.; Cui, Y.; Shi, X.; Dong, J.; Ye, M.; Li, L. Dual-Functional Ti(IV)-IMAC Material Enables Simultaneous Enrichment and Separation of Diverse Glycopeptides and Phosphopeptides. *Anal. Chem.* **2021**, *93* (24), 8568–8576.

(43) Huang, J.; Dong, J.; Shi, X.; Chen, Z.; Cui, Y.; Liu, X.; Ye, M.; Li, L. Dual-Functional Titanium(IV) Immobilized Metal Affinity Chromatography Approach for Enabling Large-Scale Profiling of Protein Mannose-6-Phosphate Glycosylation and Revealing Its Predominant Substrates. *Anal. Chem.* **2019**, 1–9.

(44) Segal, M. B. Extracellular and Cerebrospinal Fluids. *J. Inherit. Metab. Dis.* **1993**, *16* (4), 617–638.

(45) Abdi, F.; Quinn, J. F.; Jankovic, J.; McIntosh, M.; Leverenz, J. B.; Peskind, E.; Nixon, R.; Nutt, J.; Chung, K.; Zabetian, C.; Samii, A.; Lin, M.; Hattan, S.; Pan, C.; Wang, Y.; Jin, J.; Zhu, D.; Li, G. J.; Liu, Y.; Waichunas, D.; Montine, T. J.; Zhang, J. Detection of Biomarkers with a Multiplex Quantitative Proteomic Platform in Cerebrospinal Fluid of Patients with Neurodegenerative Disorders. *J. Alzheimer's Dis.* **2006**, *9* (3), 293–348.

(46) Zhang, J. Proteomics of Human Cerebrospinal Fluid – the Good, the Bad, and the Ugly. *Proteom. - Clin. Appl.* **2007**, *1* (8), 805–819.

(47) Shores, K. S.; Knapp, D. R. Assessment Approach for Evaluating High Abundance Protein Depletion Methods for Cerebrospinal Fluid (CSF) Proteomic Analysis. *J. Proteome Res.* **2007**, *6* (9), 3739–3751.

(48) Yang, K.; Yang, Z.; Chen, X.; Li, W. The Significance of Sialylation on the Pathogenesis of Alzheimer's Disease. *Brain Res. Bull.* **2021**, *173*, 116–123.

(49) Evin, G.; Li, Q.-X. Platelets and Alzheimer's Disease: Potential of APP as a Biomarker. *World J. Psychiatry* **2012**, *2* (6), 102–113.

(50) Knebl, J.; DeFazio, P.; Clearfield, M. B.; Little, L.; McConathy, W. J.; Pherson, R. M.; Lacko, A. G. Plasma Lipids and Cholesterol Esterification in Alzheimer's Disease. *Mech. Ageing Dev.* **1994**, *73* (1), 69–77.

(51) Zhong, X.; Wang, J.; Carlsson, C.; Okonkwo, O.; Zetterberg, H.; Li, L. A Strategy for Discovery and Verification of Candidate Biomarkers in Cerebrospinal Fluid of Preclinical Alzheimer's Disease. *Front. Mol. Neurosci.* **2019**, *11*, 483.

(52) McGeer, P. L.; McGeer, E. G. The Possible Role of Complement Activation in Alzheimer Disease. *Trends Mol. Med.* **2002**, *8* (11), 519–523.

(53) Roth, J. Protein N-Glycosylation along the Secretory Pathway: Relationship to Organelle Topography and Function, Protein Quality Control, and Cell Interactions. *Chem. Rev.* **2002**, *102* (2), 285–304.

(54) Zhong, X.; Yu, Q.; Ma, F.; Frost, D. C.; Lu, L.; Chen, Z.; Zetterberg, H.; Carlsson, C.; Okonkwo, O.; Li, L. HOTMAQ: A Multiplexed Absolute Quantification Method for Targeted Proteomics. *Anal. Chem.* **2019**, *91* (3), 2112–2119.

(55) Donner, L.; Fälker, K.; Gremer, L.; Klinker, S.; Pagani, G.; Ljungberg, L. U.; Lothmann, K.; Rizzi, F.; Schaller, M.; Gohlke, H.; Willbold, D.; Grenegard, M.; Elvers, M. Platelets Contribute to Amyloid- β Aggregation in Cerebral Vessels through Integrin $\text{Al}\text{IIb}\beta\text{3}$ -Induced Outside-in Signaling and Clusterin Release. *Sci. Signal.* **2016**, *9* (429), ra52–ra52.

(56) Sackmann, C.; Hallbeck, M. Oligomeric Amyloid- β Induces Early and Widespread Changes to the Proteome in Human iPSC-Derived Neurons. *Sci. Rep.* **2020**, *10* (1), 6538.

(57) PASCALE, A.; ETCHEBERRIGARAY, R. CALCIUM ALTERATIONS IN ALZHEIMER'S DISEASE: PATHOPHYSIOLOGY, MODELS AND THERAPEUTIC OPPORTUNITIES. *Pharmacol. Res.* **1999**, *39* (2), 81–88.

(58) Řípová, D.; Platilová, V.; Strunecká, A.; Jirák, R.; Höschl, C. Cytosolic Calcium Alterations in Platelets of Patients with Early Stages of Alzheimer's Disease. *Neurobiol. Aging* **2000**, *21* (5), 729–734.

(59) Chen, C. P. C.; Huang, Y.-C.; Chang, C.-N.; Chen, J.-L.; Hsu, C.-C.; Lin, W.-Y. Changes of Cerebrospinal Fluid Protein Concentrations and Gait Patterns in Geriatric Normal Pressure Hydrocephalus Patients after Ventriculoperitoneal Shunting Surgery. *Exp. Gerontol.* **2018**, *106*, 109–115.

(60) Domenico, F. D.; Pupo, G.; Giraldo, E.; Badia, M.-C.; Monllor, P.; Lloret, A.; Schininà, M. E.; Giorgi, A.; Cini, C.; Tramutola, A.; Butterfield, D. A.; Viña, J.; Perluigi, M. Oxidative Signature of Cerebrospinal Fluid from Mild Cognitive Impairment and Alzheimer Disease Patients. *Free Radic. Biol. Med.* **2016**, *91*, 1–9.

(61) Pahlsson, P.; Shakin-Eshleman, S. H.; Spitalnik, S. L. N-Linked Glycosylation of β -Amyloid Precursor Protein. *Biochem. Biophys. Res. Commun.* **1992**, *189* (3), 1667–1673.

(62) Tsatsanis, A.; Dickens, S.; Kwok, J. C. F.; Wong, B. X.; Duce, J. A. Post Translational Modulation of β -Amyloid Precursor Protein Trafficking to the Cell Surface Alters Neuronal Iron Homeostasis. *Neurochem. Res.* **2019**, *44* (6), 1367–1374.

(63) Halim, A.; Brinkmalm, G.; Rüetschi, U.; Westman-Brinkmalm, A.; Portelius, E.; Zetterberg, H.; Blennow, K.; Larson, G.; Nilsson, J. Site-Specific Characterization of Threonine, Serine, and Tyrosine Glycosylations of Amyloid Precursor Protein/Amyloid β -Peptides in Human Cerebrospinal Fluid. *Proc. Natl. Acad. Sci.* **2011**, *108* (29), 11848–11853.

(64) Boix, C. P.; Lopez-Font, I.; Cuchillo-Ibañez, I.; Sáez-Valero, J. Amyloid Precursor Protein Glycosylation Is Altered in the Brain of Patients with Alzheimer’s Disease. *Alzheimer Res. Ther.* **2020**, *12* (1), 96.

Figure Legends

Figure 1. Workflow of Boost-DiLeu strategy. Proteins from biological samples were extracted, digested and labeled through one-tube sample preparation workflow. DiLeu 118d was used as a boosting channel. Samples were pooled after labeling for HILIC enrichment and HpH fractionation, followed by LC-MS/MS analysis.

Figure 2. Comparison of sample preparation using conventional and one-tube sample processing workflow. (A) Identification number in glycoproteomic analysis. (B) Overlap of glycoproteins.

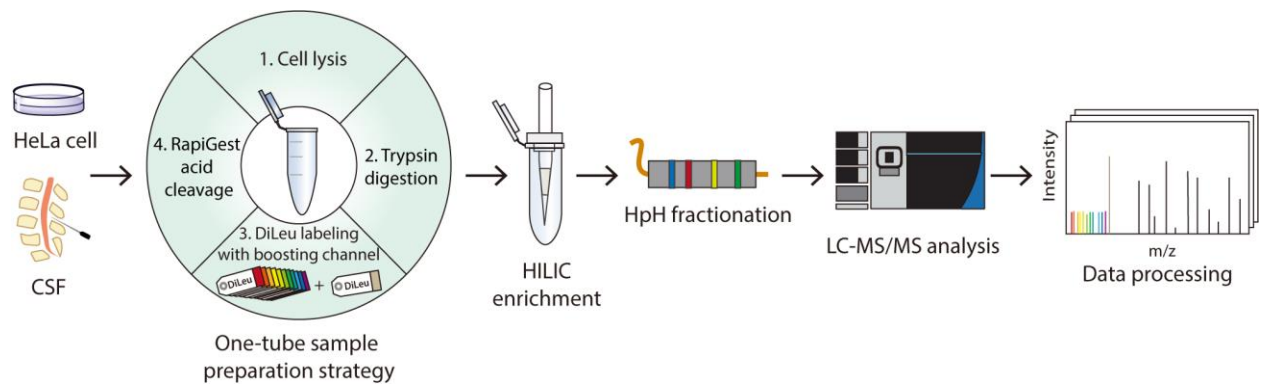
Figure 3. Comparison of different B/S ratios. (A) Experimental design: First three channels were labeled as study channels and 118d channel was used for boosting channel. (B) Reporter ion signal intensities at a 30x B/S ratio. (C) Identification number of GPSMs, total glycopeptides and quantifiable glycopeptides at different B/S ratios. (D) CV distribution of quantifiable glycopeptides.

Figure 4. Comparison of different AGC settings. (A) Identification number of GPSMs, total glycopeptides and quantifiable glycopeptides with different AGC. (B) CV distribution of quantifiable glycopeptides. (C) Distribution of reporter ion signal intensities. (D) Distribution of actual ion injection time.

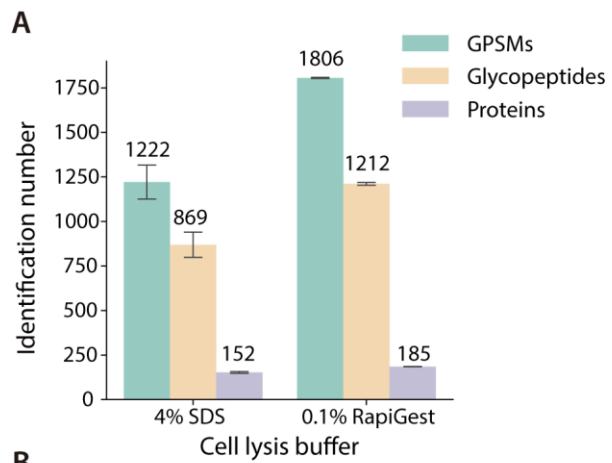
Figure 5. Global glycoproteome mapping in HeLa cell line. (A) Identification number of GPSMs, total glycopeptides and quantifiable glycopeptides. (B) Overlap of unique glycopeptides identified in each fraction. (C) A glycoprotein-glycan network maps which glycans (outer nodes) modify which proteins (inner bar). Glycoproteins are sorted by number of glycosites. (D) Distribution of reporter ion signal intensities across 12 channels. (E) CV distribution of quantifiable glycopeptides. (F) Pearson correlation of reporter ion intensities between three study channels.

Figure 6. Site-specific quantitative glycoproteomic analysis of human CSF samples. (A) 18 aberrant N-glycopeptides in AD CSF samples with site-specific information (* $p < 0.05$, ** $p < 0.01$, and *** $p < 0.001$). (B) WGCNA cluster dendrogram of 164 glycoproteins. (C) GO analysis of M1 proteins clustered in WGCNA dendrogram.

Figures

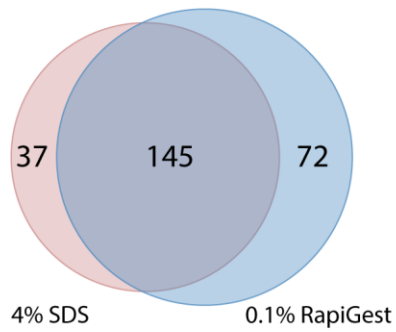


Wang et al., Figure 1.

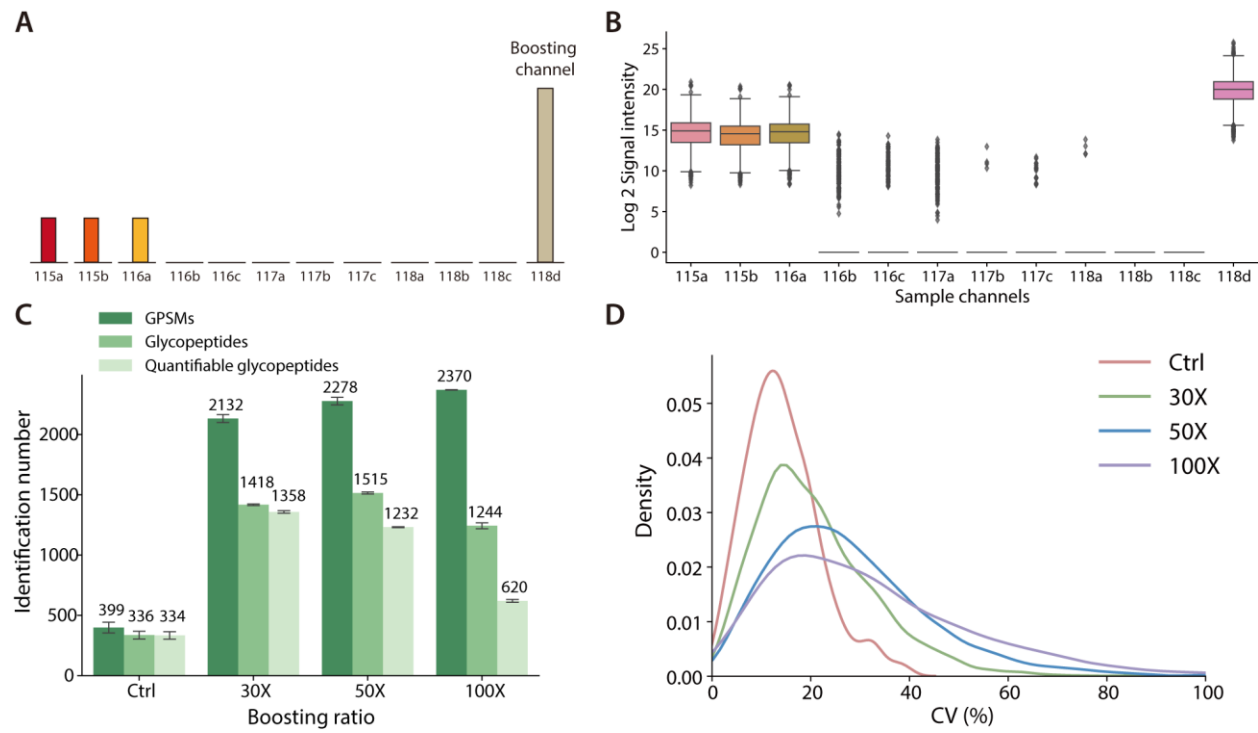


B

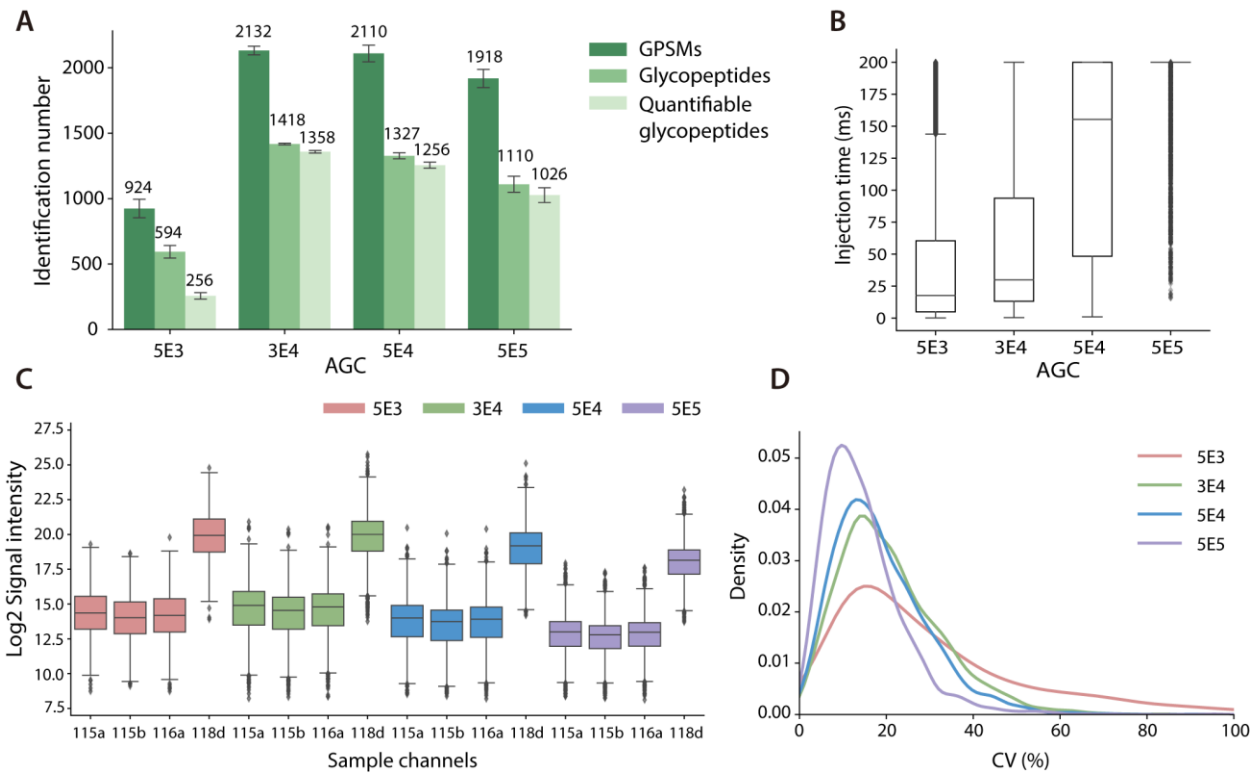
Glycoproteins



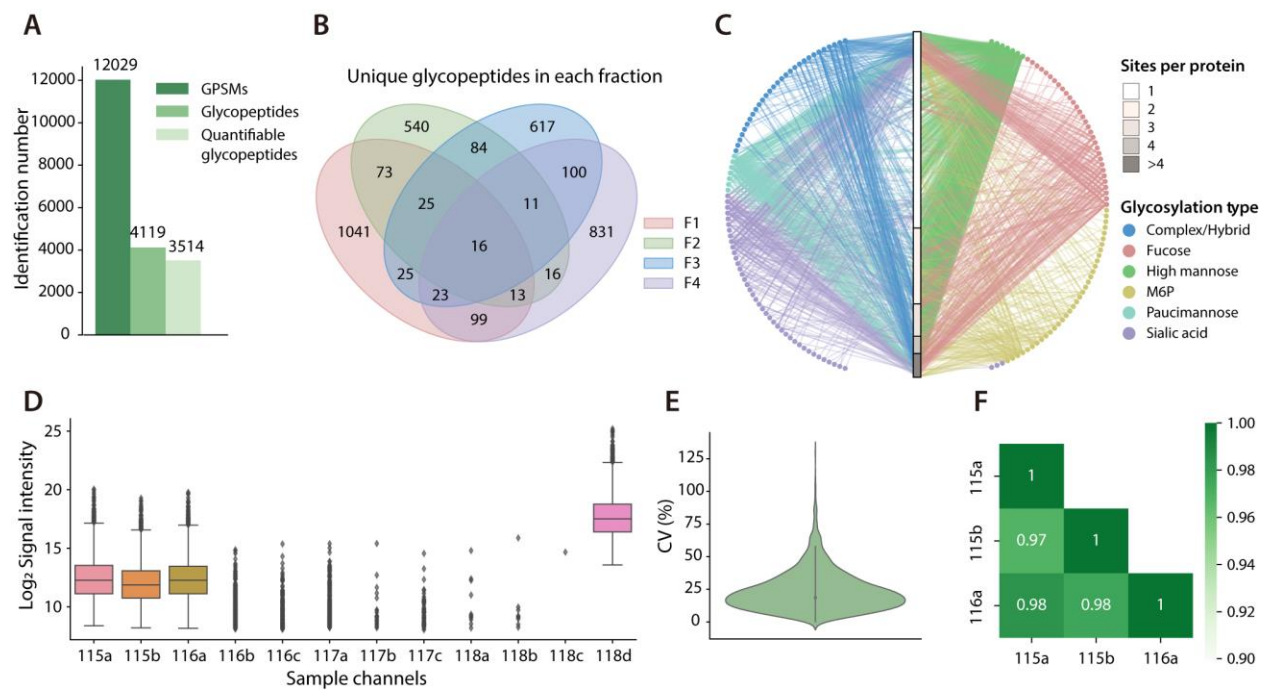
Wang et al., Figure 2.



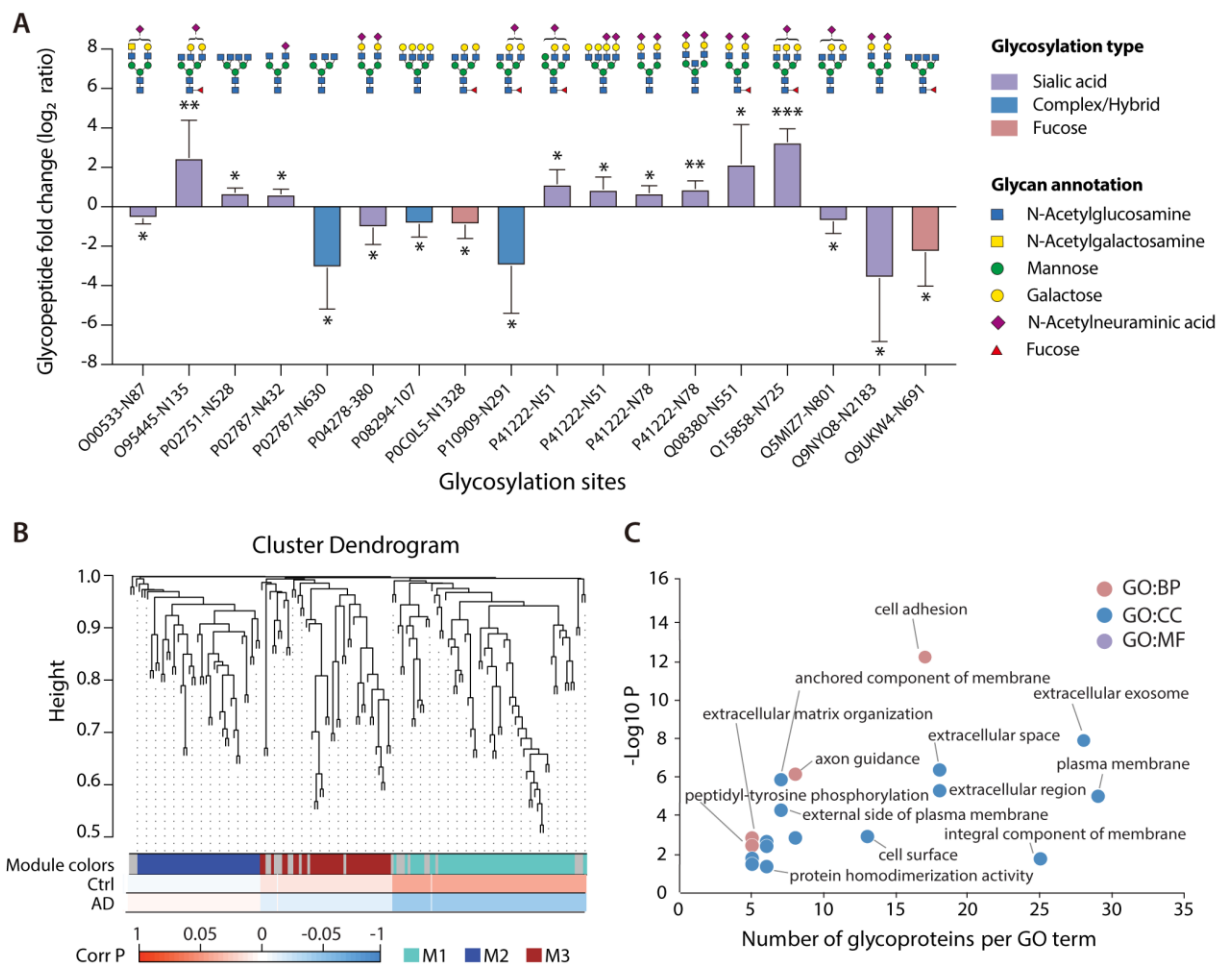
Wang et al., Figure 3.



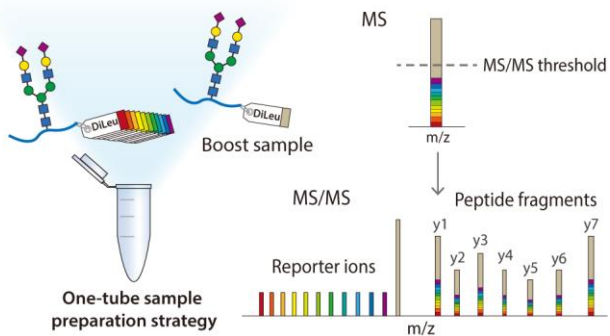
Wang et al., Figure 4.



Wang et al., Figure 5.



Wang et al., Figure 6.



Abstract Graphic